RESEARCH ARTICLE

Dysregulated Hepatic Methionine Metabolism Drives Homocysteine Elevation in Diet-Induced Nonalcoholic Fatty Liver Disease

Tommy Pacana[1]*, Sophie Cazanave[1], Aurora Verdianelli[1], Vaishali Patel[1], Hae-Ki Min[1], Faridoddin Mirshahi[1], Eoin Quinlivan[2], Arun J. Sanyal[1]*

1 Div. of Gastroenterology, Hepatology and Nutrition, Dept. of Internal Medicine, Virginia Commonwealth University School of Medicine, Richmond, VA, 23298, United States of America, 2 Biomedical Mass Spectrometry Laboratory, General Clinical Research Center, University of Florida, Gainesville, FL, United States of America

* asanyal@mcvh-vcu.edu (AJS); tpacana@mcvh-vcu.edu (TP)

Abstract

Methionine metabolism plays a central role in methylation reactions, production of glutathione and methylarginines, and modulating homocysteine levels. The mechanisms by which these are affected in NAFLD are not fully understood. The aim is to perform a metabolomic, molecular and epigenetic analyses of hepatic methionine metabolism in diet-induced NAFLD. Female 129S1/SvlmJ;C57Bl/6J mice were fed a chow (n = 6) or high-fat high-cholesterol (HFHC) diet (n = 8) for 52 weeks. Metabolomic study, enzymatic expression and DNA methylation analyses were performed. HFHC diet led to weight gain, marked steatosis and extensive fibrosis. In the methionine cycle, hepatic methionine was depleted (30%, p< 0.01) while s-adenosylmethionine (SAM)/methionine ratio (p< 0.05), s-adenosylhomocysteine (SAH) (35%, p< 0.01) and homocysteine (25%, p< 0.01) were increased significantly. SAH hydrolase protein levels decreased significantly (p <0.01). Serine, a substrate for both homocysteine remethylation and transsulfuration, was depleted (45%, p< 0.01). In the transsulfuration pathway, cystathionine and cysteine trended upward while glutathione decreased significantly (p< 0.05). In the transmethylation pathway, levels of glycine N-methyltransferase (GNMT), the most abundant methyltransferase in the liver, decreased. The phosphatidylcholine (PC)/ phosphatidylethanolamine (PE) ratio increased significantly (p< 0.01), indicative of increased phosphatidylethanolamine methyltransferase (PEMT) activity. The protein levels of protein arginine methyltransferase 1 (PRMT1) increased significantly, but its products, monomethylarginine (MMA) and asymmetric dimethylarginine (ADMA), decreased significantly. Circulating ADMA increased and approached significance (p< 0.06). Protein expression of methionine adenosyltransferase 1A, cystathionine β-synthase, γ-glutamylcysteine synthetase, betaine-homocysteine methyltransferase, and methionine synthase remained unchanged. Although gene expression of the DNA methyltransferase Dnmt3a decreased, the global DNA methylation was unaltered. Among individual genes, only HMG-CoA reductase (Hmgcr) was hypermethylated, and no methylation

changes were observed in *fatty acid synthase (Fasn)*, *nuclear factor of kappa light polypeptide gene enhancer in B-cells 1 (Nfκb1)*, *c-Jun*, *B-cell lymphoma 2 (Bcl-2) and Caspase 3*. NAFLD was associated with hepatic methionine deficiency and homocysteine elevation, resulting mainly from impaired homocysteine remethylation, and aberrancy in methyltransferase reactions. Despite increased PRMT1 expression, hepatic ADMA was depleted while circulating ADMA was increased, suggesting increased export to circulation.

Introduction

Nonalcoholic fatty liver disease (NAFLD) is the most common cause of chronic liver disease in many parts of the world [1]. It is closely linked to the associated presence of insulin resistance and the metabolic syndrome [2, 3]. The clinical-histological phenotype of NAFLD extends from nonalcoholic fatty liver (NAFL) to nonalcoholic steatohepatitis (NASH). NAFLD is associated with increased mortality [4]; cardiovascular-, liver- and cancer-related deaths account for this excess mortality [5, 6]. The pathogenesis of NAFLD is only incompletely understood.

Methionine is an essential amino acid and plays a key role as a regulator of several cellular functions [7, 8]. Its metabolism takes place mainly in the liver [9]. It is converted to s-adenosylmethionine (SAM), the primary source of methyl groups, required for transmethylation reactions and needed for the synthesis of phosphatidylcholine, creatine, sarcosine and methylarginines [10, 11]. Enzymes that catalyze DNA methylation also utilize the methyl group from SAM. Demethylation of SAM converts it sequentially to s-adenosylhomocysteine (SAH) and homocysteine [12]. Homocysteine can be remethylated to methionine or used for transsulfuration reactions that generate glutathione [13]. Hyperhomocysteinemia is associated with the metabolic syndrome and NAFLD [14–16] and has been associated with oxidative stress, inflammation, unfolded protein response, cell death and increased cardiovascular risk [17–20]. These pathways are all currently believed to be important in the pathogenesis of NASH [21]. The mechanism(s) by which hyperhomocysteinemia develops in NAFLD is not well understood.

There are only limited data on the impact of diet-induced obesity and development of NAFLD on methionine metabolism and how that impacts levels of homocysteine, ability to replenish glutathione, form biologically active methylarginines and the methylation status of key targets involved in the pathogenesis of NASH. The existing literature has focused mainly on early time points (3–12 weeks) following a high-fat diet and most have focused on selected metabolic pathways [22–25]. While some have shown SAM depletion [22, 23], others have been unable to demonstrate such changes at these early time points when steatosis is present but where the disease has not progressed to bridging fibrosis or cirrhosis [24, 25]. Thus, the status of hepatic methionine metabolism in diet-induced obesity and advanced NAFLD remains to be clarified.

The objective of the current study was to define the status of methionine metabolic pathways and production of key downstream metabolites in diet-induced obesity and NAFLD using a combined metabolomic and molecular approach. The study was performed in a mouse model of NAFLD which progressed to advanced fibrosis after 52 weeks of high-fat high-cholesterol (HFHC) diet.

Methods

Mice and diets

Female 129S1/SvlmJ;C57Bl/6J mice were kindly provided by Dr. Sandra Erickson (UCSF, CA) and kept on a 12:12-h light-dark cycle. At 10 weeks of age, the mice were randomly assigned to two groups: chow (n = 6) and HFHC diet group (n = 8). The chow group was fed a standard chow diet (Teklad 7012, Harlan) with 17% of energy derived from fat, 58% from carbohydrates, and 25% from protein; HFHC group received a western diet (Teklad 88137, Harlan) with 42% of energy derived from fat, 43% from carbohydrate, and 15% from protein. Food and water were provided ad libitum for 52 weeks until sacrifice. At the end of the feeding period, the animals were fasted for 12 hours, euthanized by CO_2, and body weights determined. Blood was collected through heart puncture, allowed to clot, and serum obtained by centrifugation at 3,000 rpm for 15 minutes at 4°C. Livers were harvested, weighed, and dissected; a portion of fresh tissue was fixed in 10% buffered formalin and remaining tissues were snap-frozen in liquid nitrogen. Serum and liver samples were stored at -80°C until RNA and protein isolation or biochemical analyses. All animal experiments were approved by Institutional Animal Care and Use Committee of Virginia Commonwealth University.

Serum biochemistry profile

Serum measurements of aspartate aminotransferase (AST), alanine aminotransferase (ALT), alkaline phosphatase (ALP), gamma-glutamyltransferase, bilirubin, cholesterol, high-density lipoprotein (HDL), low-density lipoprotein (LDL), and triglycerides were performed in the clinical chemistry laboratories of the author's institution using established commercially available methods.

Histology

Liver sections were fixed in 10% formalin. Tissues were embedded in paraffin blocks and stained with hematoxylin and eosin (HE) and Masson's trichrome stain using standard commercially available methods. Steatosis, inflammation and fibrosis were quantified separately.

RNA extraction and real-time reverse transcription PCR

Primers were designed using Beacon Designer software (Bio-Rad Laboratories, Inc.), verified by BLAST search and prepared by the Nucleic Acid Core facility at Virginia Commonwealth University (S1 Table). Total RNA was isolated from the liver with a commercial RNA isolation kit (Trizol, Invitrogen) in accordance with the manufacturer's instructions (Invitrogen, CA) and purified with RNase-free DNase. cDNA was synthesized from 4 μg of total RNA by using Maloney-murine leukemia virus reverse transcriptase and oligo(dT) primers and subjected to PCR by the manufacturer's instructions. Quantitative RT-PCR was performed by SYBR Green PCR master mix (BioRad, Hercules, CA) on an ABI Prism 7300 Sequence Detection System as previously described [26]. GAPDH was used as the endogenous normalizer. Cycle threshold (Ct) values were normalized to GAPDH and comparative quantification of target mRNA was done by ΔΔCt method using integrated software with Stratagene Mx3000P QPCR system.

Protein extraction and western blot analysis

Mouse liver tissues were lysed using RIPA lysis buffer (Sigma, St. Louis, MO) and subjected to sonication on ice with a Sonicator cell disrupter, Model 100 Sonic Dismembrator (Thermo Fisher Scientific Inc., Waltham, MA). Cell lysates were centrifuged at 12,000 g x 15mins, supernatants collected, and separated using 4%–12% NuPAGE Novex Bis-Tris Mini Gels (Invitrogen) and transferred to a nitrocellulose membrane for 1 hr at 40V using a Western blot

apparatus (Invitrogen). After overnight incubation with primary antibody, membranes were washed, incubated with HRP-conjugated secondary antibodies (Pierce Biotechnology, Inc., Rockford, IL) and detected using the SuperSignal chemiluminescence kit (Pierce). The signal capture and protein level analyses were performed as described before [27].

Standards and stable isotope labeled standards

Asymmetric-dimethylarginine (ADMA) and symmetric-dimethylarginine (SDMA) were purchased from Axxora LLC (San Diego, CA). Methylarginine (NG-mono-methyl-arginine) was purchased from Acros Organics (New Jersey). S-adenosyl-homocysteine (SAH) was purchased from Cayman Chemical Co. (Ann Arbor, MI). S-adenosyl-methionine (SAM) was purchased from New England Biochemicals (Ipswich, MA). The remaining standards were purchased from Sigma-Aldrich (St Louis, MO).

The following isotopically labeled standards [N,N-methyl-^{2}H$_6$]dimethylglycine, [2,3,3-^{2}H$_3$] serine, [U-^{13}C]methionine, [1,2-^{13}C$_2$]glycine, [guanido-^{15}N$_2$]arginine, [^{2}H$_{11}$]betaine, [methyl-^{2}H$_3$]sarcosine, [methyl-^{2}H$_3$]creatine, [methyl-^{2}H$_3$]creatinine, 2,2-^{2}H$_2$]guanidineacetic acid, [2,3,3,4,4,5,5-^{2}H$_7$]ornithine, [trimethyl-^{2}H$_9$]choline chloride and [3,3,4,4-^{2}H$_4$]cystathionine were purchased from Cambridge Isotopes (Andover, MA). [methyl-^{2}H$_3$]SAM was purchased from CDN Isotopes (Pointe-Claire, Quebec, Canada). [3,3',4,4'-^{2}H$_4$]SAH was purchased from Cayman Chemical Co. (Ann Arbor, MI). [U-13C]methionine sulfoxide was synthesized by oxidizing [U-13C]methionine with hydrogen peroxide. [^{2}H$_7$]methylarginine, [^{2}H$_7$]ADMA and [^{2}H$_7$]SDMA were each synthesized from [2,3,3,4,4,5,5-^{2}H$_7$]ornithine. A stock internal standard solution was prepared by diluting the isotopically labeled compounds, except [^{2}H$_3$]SAM and [^{2}H$_4$]SAH, in water. The [^{2}H$_3$]SAM and [^{2}H$_4$]SAH stock solutions were prepared freshly, by dissolving the solid compounds in 100 mM HCl, and mixing at the appropriate concentration with the other internal standards.

Measurement of one-carbon metabolite concentrations

Just prior to homogenization, acetic acid (100 mmol/L) containing the labeled internal standards was added to the liver sample (20 mg each). The volume of internal standard mixture added was equal to 10 µl per mg of weighed tissue (200 µl per 20 mg tissue). The sample was then homogenized using a Pellet pestel (Kontes).

To precipitate proteins, 150 µl ice cold methanol was added to 50 µl homogenate. After vortexing to mix, the sample was centrifuged at 20,000 g for 5 min. The supernatant was then analyzed by LC-MS/MS using a Thermo-Finnigan Quantum Ultra in SRM mode. The ratio of each analyte to its internal standard was calculated and the analyte concentration was determined by comparing against standard calibration curves.

Measurement of homocysteine, cysteine, glutathione and cysteinyl-glycine concentrations

Total homocysteine, cysteine, glutathione and cysteinyl-glycine concentrations were measured after reducing to free thiols and derivatizing by HPLC with fluorescence detection as previously described [28].

Measurement of phosphatidylethanolamine and phosphatidylcholine concentrations

The liver tissue samples were weighed, pulverized with the CP02 CryoPrep Dry Pulverization System (Covaris), and resuspended in ice-cold methanol containing 0.1% butyl-hydroxy-

toluene (BHT) in a concentration of 100 mg/ml. Phospholipids were extracted using a modified Folch lipid extraction [29] performed on a Hamilton Microlab Star robot. Samples were spiked with known amounts of non-endogeneous synthetic internal standards as described by Ståhlman et al. [30]. After lipid extraction, samples were reconstituted in chloroform:methanol (1:2, v/v). The extracts were stored at -20°C prior to MS analysis.

The lipid extracts were analyzed on a hybrid triple quadrupole/linear ion trap mass spectrometer (QTRAP 5500) equipped with a robotic nanoflow ion source (NanoMate HD) according to Ståhlman and colleagues [30]. Molecular lipids were analyzed in both positive and negative ion modes using multiple precursor ion scanning (MPIS) and neutral loss (NL) based methods [31, 32]. Lipids were normalized to their respective internal standard and the tissue weight.

Determination of percentage deoxycytidine methylation

Genomic DNA was extracted from 10 mg of liver using a DNeasy Blood and Tissue Kit (Qiagen, Germantown, MD) according to the manufacturer's instructions. After adding biosynthetic $[^{15}N_3]dC$ and $[^{15}N_3]5mdC$ internal standards [33] to the liver DNA, the DNA was digested to nucleosides [33, 34]. The concentrations of deoxycytidine and 5-methyldeoxycytidine (5mdC) were determined by LC-MS/MS [33]. Percentage deoxycytidine methylation (% 5mdC) was calculated as: % 5mdC = [5mdC] / ([dC] + [5mdC]) x 100. Inter- and intra-assay variation (relative standard deviation; n = 6) for the assay was < 2.5%.

Determination of relative 5-hydroxymethyl-2'-deoxycytidine concentrations

Labeled $[^{15}N_3]$ standards for 5-hydroxymethyl-2'-deoxycytidine (5hmdC) analysis were biosynthesized from $[^{15}N_3]DNA$ and formaldehyde, after which it was digested to nucleosides. The resulting $[^{15}N_3]dC$ and $[^{15}N_3]5hmdC$ was added to the samples of liver DNA, and the DNA digested to nucleosides and analyzed by LC-MS/MS [34]. The mass transitions used for 5hmdC and $[^{15}N_3]5hmdC$ were 258→142 and 261→145, respectively. As we did not have an authentic 5hmdC standard for determining absolute 5hmdC concentrations, relative 5hmdC concentration (relative to dC) were calculated from the analyte and internal peak areas: Relative 5hmdC conc. = (5hmdC / $[^{15}N_3]5hmdC$) ÷ (dC / $[^{15}N_3]dC$). These are arbitrary units. The intra-assay variation (relative standard deviation; n = 6) for the assay was < 6%.

DNA methylation status of HMGCR, FASN, NFkB1, c-Jun, Bcl-2 and Caspase 3

DNA methylation analyses of promoter CpG islands for 3-hydroxy-3-methylglutaryl-coenzyme A reductase (*Hmgcr*) and fatty acid synthase (*Fasn*), nuclear factor of kappa light polypeptide gene enhancer in B-cells 1 (*Nfkb1*), c-Jun, B-cell lymphoma 2 (*Bcl-2*) and Caspase 3 targets were performed by EpiTect® Methyl II PCR arrays (Qiagen, Frederick, MD) using a methylation-sensitive and/or methylation-dependent restriction enzyme digestion, followed by SYBR Green real-time PCR detection. Using the ΔCt method, the relative amount of methylated and unmethylated DNA fractions were calculated by comparing the amount in each digest with that of a mock (no enzymes added) digest.

Statistical analysis

The levels of specific metabolites in chow-fed versus HFHC diet-fed mice were compared using unpaired Student's T-test or Kruskal Wallis analysis of variance as appropriate. Data are

presented as the mean ± standard error of the mean (SEM). Given a standard deviation of 20% of the mean, a sample of 7 in each group was estimated to be able to detect a 25–30% change across groups with a power of 80%. A p value of < 0.05 was considered to be significant.

Results

Morphology, biochemical profile and histology

A total of 6 and 10 mice were given either chow diet or HFHC diet, respectively, for 52 weeks. Two mice died between week 32–40 and a total of 8 and 6 mice receiving HFHC or chow diet, respectively, survived to the end of study. Mice fed with HFHC diet significantly gained more body weight (50.5 g vs 36.7 g; p< 0.01) and liver weight (2.4 g vs 1.3 g; p< 0.05) than mice fed with chow diet at 52 weeks (Table 1). HFHC diet also led to significantly increased serum aminotransferases, cholesterol, triglycerides, HDL, LDL and HOMA-IR. Histological examination of the liver confirmed the presence of steatosis, involving over 75% of the liver in mice fed a HFHC diet (S1 Fig). The steatosis was panacinar and included both macrovesicular and small droplet steatosis. Sheets of cells with small droplet steatosis, predominantly centrilobular in distribution, were seen. There were also scattered foci of inflammatory cells and extensive pericellular fibrosis (S1 Fig).

HFHC diet induces multiple changes in the methionine cycle

A: Methionine depletion, increased SAM/methionine ratio, SAH elevation and excess homocysteine in the liver with HFHC diet. The first step in the methionine cycle is demethylation of methionine to SAM via methionine adenosyltransferase (MAT). MAT is the product of two different genes, *Mat1a* and *Mat2a*. The former is expressed only in adult hepatocytes while the latter is expressed both in hepatic and extrahepatic tissues [35]. HFHC diet led to 30% depletion of methionine (p< 0.01) and a modest non-significant increase in SAM. The SAM/methionine ratio increased significantly (p< 0.05) (Fig 1A and 1B). To determine whether the observed decrease in methionine was due to its conversion to oxidative

Table 1. Morphological and biochemical profile at 52 weeks of chow and HFHC diet.

	Chow (n = 6)	HFHC (n = 8)	P-value
Body weight (gram)	36.7 ± 2.4	50.5 ± 3.0	<0.05
Liver weight (gram)	1.3 ± 0.1	2.4 ± 0.4	<0.05
Insulin (mU/l)	48.4 ± 5.1	65.5 ± 8.7	<0.05
HOMA-IR	43.6 ± 5.8	61.78 ± 8.2	<0.05
AST (unit/L)	220.8 ± 57.6	628.4 ± 83.6	<0.01
ALT (unit/L)	58 ± 6.0	560.5 ± 127.5	<0.01
ALP (unit/L)	40.5 ± 8.9	132.0 ± 26.0	<0.05
GGT (unit/L)	<0.5	<0.5	NA
Bilirubin (mg/dl)	<0.1	<0.1	NA
Cholesterol (mg/dl)	128.8 ± 10.6	337.4 ± 40.2	<0.01
HDL (mg/dl)	54.3 ± 4.4	105.8 ± 6.5	<0.01
LDL (mg/dl)	56.0 ± 6.3	209.8 ± 33.3	<0.01
Triglyceride (mg/dl)	92.7 ± 1.1	110.9 ± 2.6	<0.05

Data are represented as mean ± SEM. aspartate aminotransferase, AST; alanine aminotransferase, ALT; alkaline phosphatase, ALP; gamma-glutamyltransferase, GGT; high-density lipoprotein, HDL; high-fat high-calorie, HFHC; homeostasis model assessment of insulin resistance, HOMA-IR; low-density lipoprotein, LDL
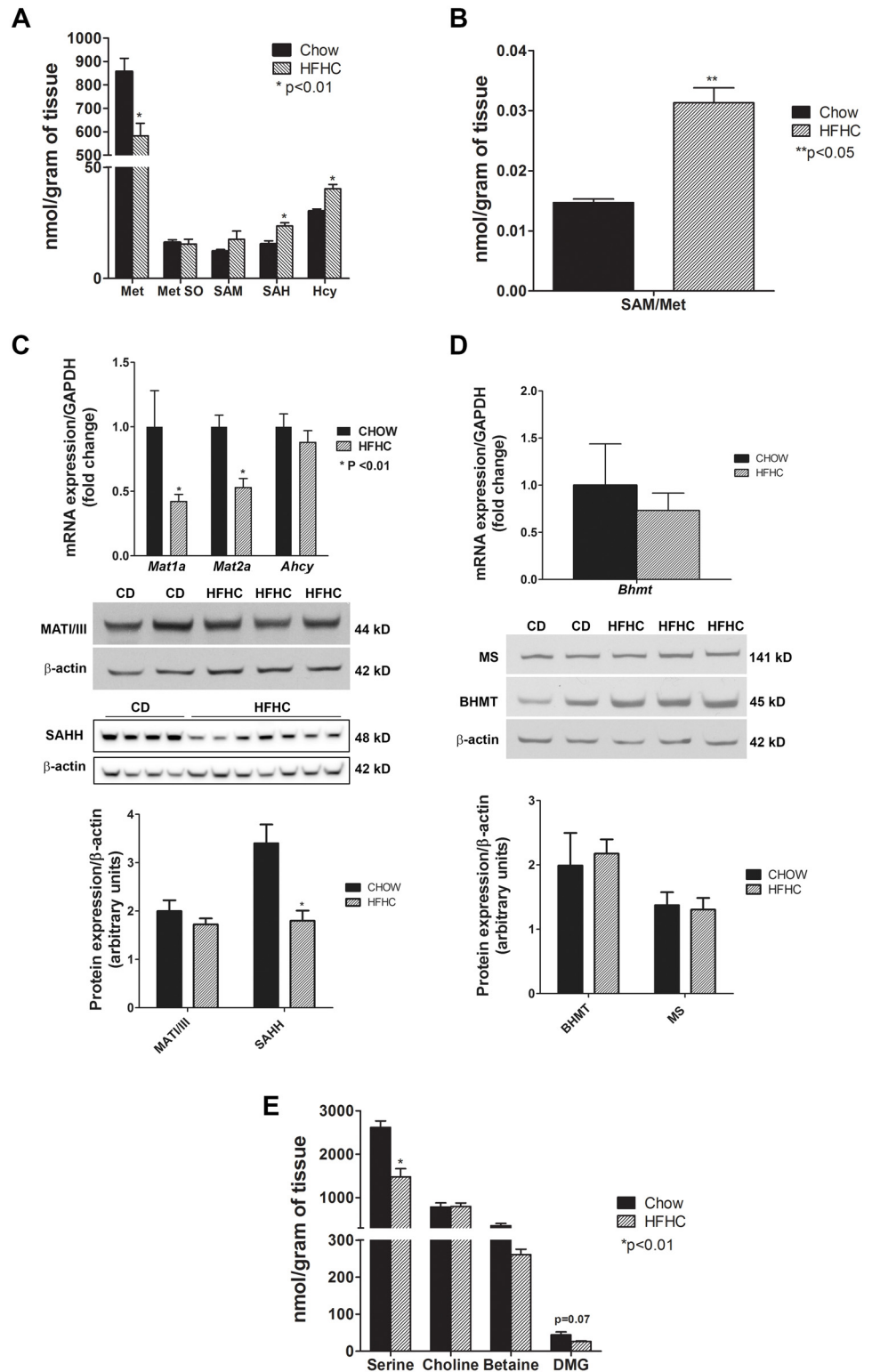
doi:10.1371/journal.pone.0136822.t001

Fig 1. Methionine cycle: hepatic methionine depletion and homocysteine accumulation in diet-induced NAFLD. (A) HFHC diet for 52 weeks resulted in methionine (met) depletion (p< 0.01) and increased downstream products s-adenosylmethionine (SAM), s-adenosylhomocysteine (SAH) (p< 0.01) and homocysteine (Hcy) (p< 0.01) and (B) increased SAM/methionine ratio (p< 0.05), which is indicative of increased methionine utilization. Methionine sulfoxide (Met So) concentration remained unchanged. (C) The

gene expression of methionine adenosyltransferase *Mat1a* and *Mat2a* was decreased (p< 0.01). However, the protein levels of MAT I/III, expressed solely by hepatic *Mat1a*, were relatively unchanged. Although *SAH hydrolase* (*Ahcy*) mRNA levels did not change, SAHH protein expression was decreased significantly (p< 0.01) which correlated with the increase in SAH levels but not the excess in Hcy. (D) The gene expression of *betaine-homocysteine methyltransferase* (*Bhmt*) and protein levels of BHMT and methionine synthase (MS), enzymes responsible for conversion of homocysteine to methionine, did not change. (E) Serine, the main one-carbon donor in the folate cycle needed for homocysteine remethylation, was depleted (p< 0.01). Whereas betaine levels trended down modestly, the decrease in dimethylglycine (DMG) almost approached significance (p = 0.07) that further indicates impairment of methionine reformation. Together, these findings suggest that homocysteine accumulation mainly results from impaired homocysteine remethylation to methionine. Data are represented as mean ± SEM.

doi:10.1371/journal.pone.0136822.g001

metabolites, methionine sulfoxide was also quantified. The levels of methionine sulfoxide did not change significantly (Fig 1A). Both the gene expressions of *Mat1a*, which encodes for MATI/III, and *Mat2a* were significantly decreased (Fig 1C). However, MAT I/III protein levels were relatively unchanged. The concentrations of SAH, the downstream product of SAM-derived transmethylation reactions, was elevated in HFHC group by 1.5 fold (p< 0.01) (Fig 1A). The protein levels of SAH hydrolase (SAHH), the enzyme that catalyzes the breakdown of SAH to homocysteine, were decreased significantly (p = 0.0022) (Fig 1C). On the other hand, the concentration of homocysteine was increased significantly (Fig 1A).

B: Metabolomic evidence of impaired remethylation of homocysteine to methionine. Homocysteine is remethylated to methionine via methionine synthase or via betaine-homocysteine methyltransferase. Methionine synthase activity requires serine-dependent activity of the folate cycle as a donor of methyl groups from methyltetrahydrofolate [36]. Despite a high homocysteine, methionine levels were low as noted above. The protein expression of methionine synthase remained unchanged on a HFHC diet (Fig 1D). However, there was a profound depletion of serine (p< 0.01) (Fig 1E), which is expected to impair the activity of the folate cycle. The levels of choline, the precursor of betaine, were not significantly altered. Whereas betaine levels trended down modestly, although non-significant, the levels of dimethylglycine, the downstream product of betaine-homocysteine methyltransferase (BHMT) activity, were even further decreased (p = 0.07) resulting in a decrease in dimethylglycine:betaine ratios. The gene and protein expression of BHMT was relatively unchanged with HFHC diet (Fig 1D).

The transsulfuration pathway is preserved after a HFHC diet

Another mechanism to remove homocysteine is through the transsulfuration pathway by conversion of homocysteine to cystathionine by cystathionine β-synthase. Cystathionine is then converted to cysteine for GSH synthesis via γ-glutamylcysteine synthetase. There was a modest non-significant increase in the levels of cystathionine and cysteine in mice on the HFHC diet (Fig 2A). However, this was not proportional to the increase in homocysteine and the homocysteine:cystathionine and homocysteine:cysteine ratios trended downwards in obese mice with NAFLD. This could be influenced by the depletion of the substrate serine, which is also needed to convert cystathionine from homocysteine, as noted above. Both *cystathionine β-synthase* and *γ-glutamylcysteine synthetase* mRNA levels decreased significantly in mice with NAFLD (Fig 2B). The protein levels of these enzymes also trended down but these changes were not significant. There was a significant decrease in the glutathione levels (p< 0.05) (Fig 2C) which is an indication of oxidative stress. The levels of cysteinyl-glycine remained unchanged. The ratio of reduced to oxidized glutathione trended upward, suggesting enhanced formation of glutathione to replete glutathione stores.
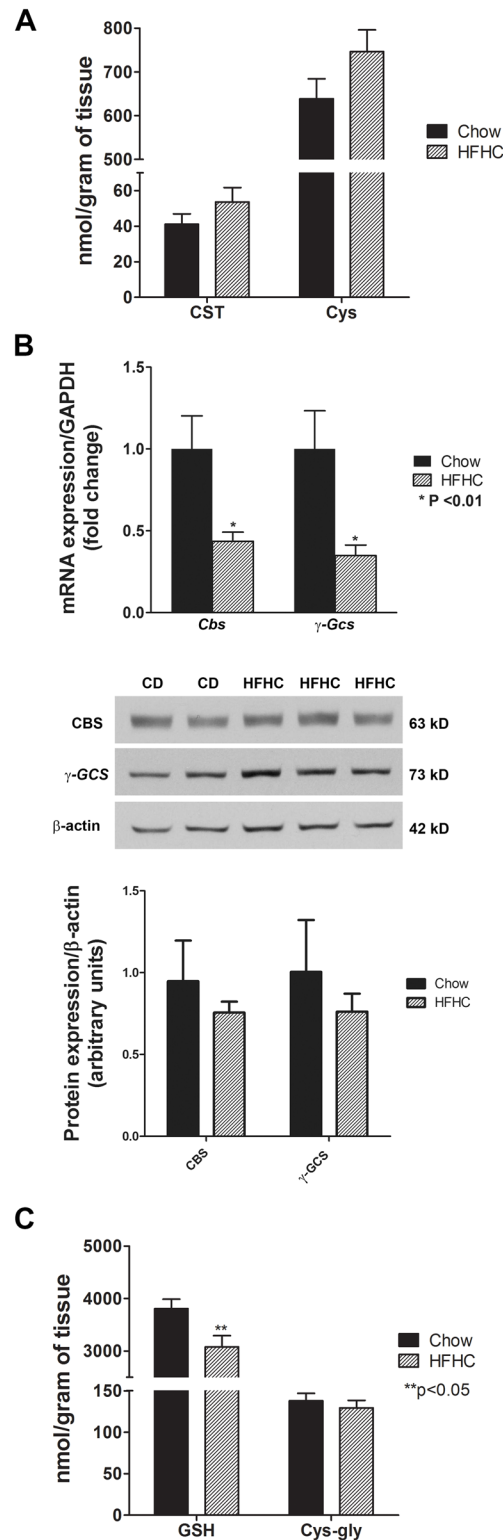
Fig 2. Transsulfuration pathway: depletion of serine limits the ability to replete glutathione in diet-induced NAFLD. (A) HFHC diet for 52 weeks resulted only in modest non-significant increase in cystathionine (CST) and cysteine (Cys) levels in spite of homocysteine accumulation and decrease in glutathione levels. (B) mRNA expression of *cystathionine β-synthase* (*Cbs*) and *γ-glutamylcysteine synthetase* (*γ-Gcs*) decreased but the protein levels of CBS and GCS did not significantly change. (C)

Glutathione (GSH) was depleted (p< 0.05), likely as a result of oxidative stress, while cysteinyl-glycine, a catabolic product of GSH, remained unchanged (C). Data are represented as mean ± SEM.

Differential changes in transmethylation pathways

Substrates and methylated products of major methyltransferase reactions were quantified: glycine and sarcosine via glycine N-methyltransferase (GNMT); phosphatidylethanolamine (PE) and phosphatidylcholine (PC) via phosphatidylethanolamine methyltransferase (PEMT); guanidinoacetate (GAA) and creatine via guanidinoacetate methyltransferase (GAMT); and arginine and monomethylarginine (MMA), symmetric dimethylarginine (SDMA) and ADMA via protein arginine methyltransferase (PRMT) (Fig 3A).

For the GNMT reaction, the concentration of glycine (the substrate) was significantly reduced while the concentration of sarcosine (the product) did not change significantly in mice with NAFLD (Fig 3B). The gene and protein levels of GNMT were decreased (Fig 3C). For the PEMT reaction, PE was reduced significantly in HFHC group (p< 0.01); however, levels of PC were not changed significantly, thus increasing the PC/PE ratio significantly (p< 0.01) (Fig 3D). There were no significant concentration differences for GAA and creatine, the substrate and product for GAMT.

The products of arginine methylation via PRMT include MMA, SDMA, and ADMA. While the levels of arginine were unchanged, MMA and ADMA were significantly reduced (p< 0.01 and p< 0.05, respectively) and SDMA reduction almost reached statistical significance (p = 0.07) with HFHC diet (Fig 3E). Due to these changes, further investigation was carried out to measure the expression of PRMT1, which is responsible mainly for the methylation of MMA and ADMA [11]. While *Prmt*1 mRNA was decreased, the protein levels for this enzyme were significantly increased (p< 0.05) (Fig 3F). Circulating ADMA levels increased and approached significance (p = 0.06) (Fig 3G).

HMG-CoA reductase DNA hypermethylation and stable global DNA methylation and hydroxymethylation with HFHC diet

The methyl groups of SAM are also used by DNA methyltransferases to methylate DNA that can lead to epigenetic modifications. The status of global DNA methylation and hydroxymethylation was determined in both groups of mice. Although the mRNA expression of *Dnmt1* and *Dnmt3a*, respectively, tended to decrease or decreased significantly (Fig 4A), there were no differences in percent 5-methyldeoxycytidine between the chow and HFHC group (Fig 4B). No differences in relative 5-hydroxymethyl-2'-deoxycytidine (5hmdC) concentrations was also observed (Fig 4C). We also investigated the methylation status of individual genes, which play important roles in the pathogenesis of human NAFLD, at promoter CpG islands for lipogenic (HMG-CoA reductase, HMGCR; and fatty acid synthase, FASN), inflammatory (NFkB1and c-Jun), and apoptosis (Bcl-2 and Caspase 3) targets. There was a significant increase in *Hmgcr* methylation in HFHC group (p<0.01), whereas no methylation changes for *Fasn*, *Nfκb1*, *c-Jun*, *Bcl-2*, and *Caspase 3* were observed (Fig 4D).

Discussion

The current study demonstrates that with long-term (52 week) feeding of a HFHC diet and development of advance NAFLD with fibrosis, there is a depletion of methionine along with an increase in its downstream products SAM, SAH and homocysteine (Fig 5). The decrease in methionine, an essential amino acid, may reflect a dietary deficiency or increase in its utilization. In the mouse model studied, the methionine concentration in the HFHC diet was higher
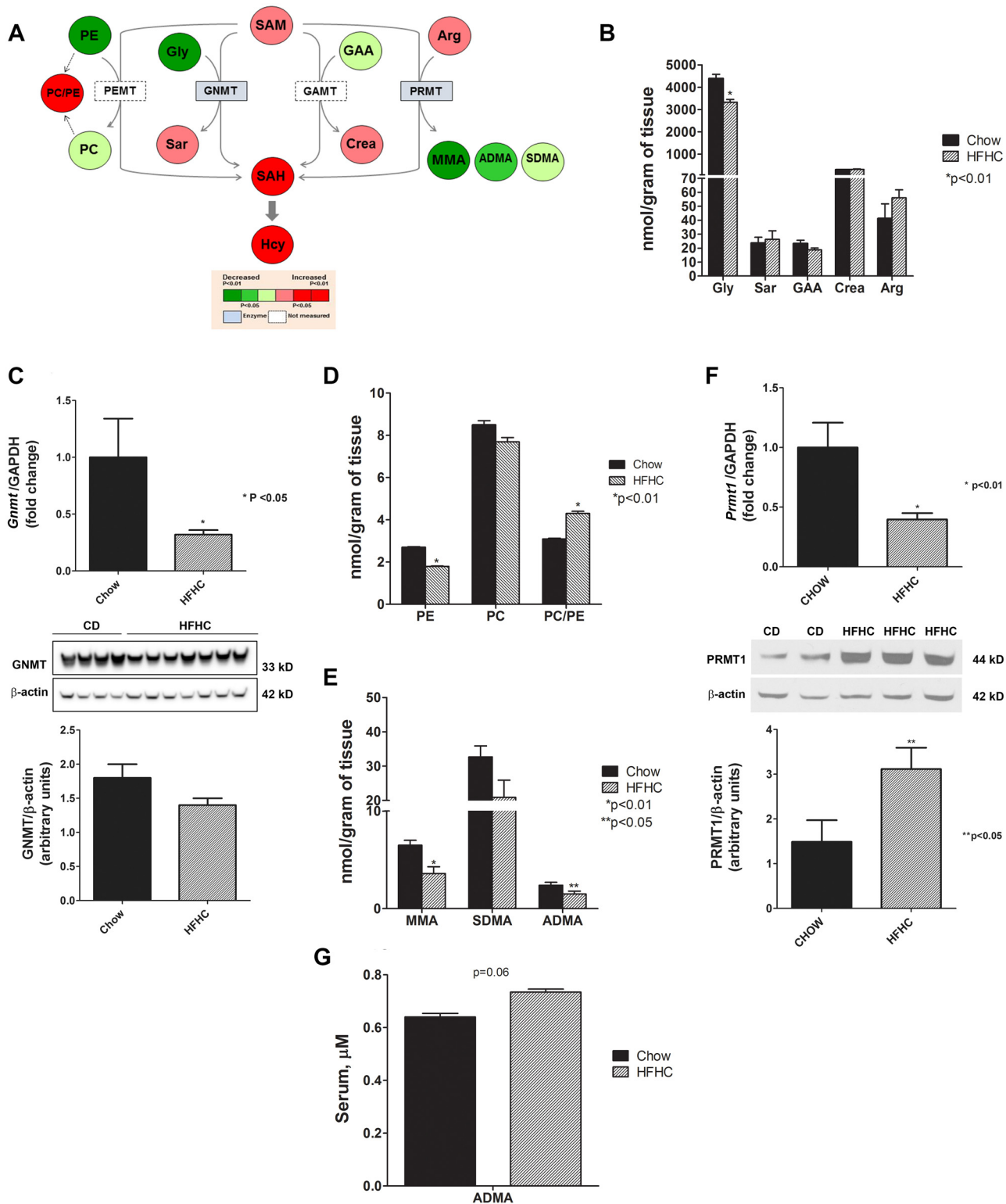
Fig 3. Transmethylation pathway: aberrancy in methyltransferase reactions in diet-induced NAFLD. (A) Heat map representation of substrates and methylated products of major SAM-derived transmethylation reactions (PEMT, GNMT, GAMT and PRMT) with HFHC diet for 52 weeks. (B) Levels of glycine, a substrate for GNMT, were decreased ($p < 0.01$) while the product sarcosine did not change between chow and HFHC group. (C) The gene expression of *Gnmt*, the most abundant methyltranserase in the liver, decreased significantly but only approached significance at the protein level ($p = 0.06$). (D) Levels of PE, the substrate for PEMT, was significantly reduced ($p < 0.01$) while PC trended down, resulting in a significant PC/PE ratio ($p < 0.01$), which suggests

increase in PEMT activity There were no significant changes in the concentrations of guanidinoacetate and creatine, the substrate and product for GAMT, respectively. (E) The methylated products of PRMT activity, MMA and ADMA, were decreased significantly (p< 0.01 and p< 0.05) while the decrease in SDMA approached significance (p = 0.07). (F) The gene expression of *Prmt1*, mainly responsible for the methylation of MMA and ADMA, decreased (p< 0.01) but the protein levels of PRMT1 increased significantly (p< 0.05). (G) Circulating ADMA was increased toward significance (p = 0.06), suggesting increased export to the circulation. Data are represented as mean ± SEM. Legend: arginine (Arg); asymmetric dimethylarginine (ADMA); creatine (Crea); glycine (Gly); glycine N-methyltransferase (GNMT); guanidinoacetate (GAA); guanidinoacetate methyltransferase (GAMT); homocysteine (Hcy); monomethylarginine (MMA); phosphatidylcholine (PC); phosphatidylethanolamine (PE); phosphatidylethanolamine methyltransferase (PEMT); protein arginine methyltransferase (PRMT); s-adenosylhomocysteine (SAH); s-adenosylmethionine (SAM); sarcosine (Sar); symmetric dimethylarginine (SDMA).

than in chow diet (7 mg/kg vs 3 mg/kg) and it is therefore unlikely that the observed decrease reflected a dietary deficiency. It is therefore inferred that the metabolic stress imposed by a HFHC diet increases demand for methionine-derived metabolites and accounts for a decrease in hepatic methionine concentration.

The depletion of hepatic methionine stores appears to be a time-dependent phenomenon. Prior studies did not find evidence of methionine depletion after 3–12 weeks of a HFHC diet [22–25]. The methionine content of the diet was not however reported and the animals only had early stage disease with steatosis without demonstrable fibrosis. The time-dependency of
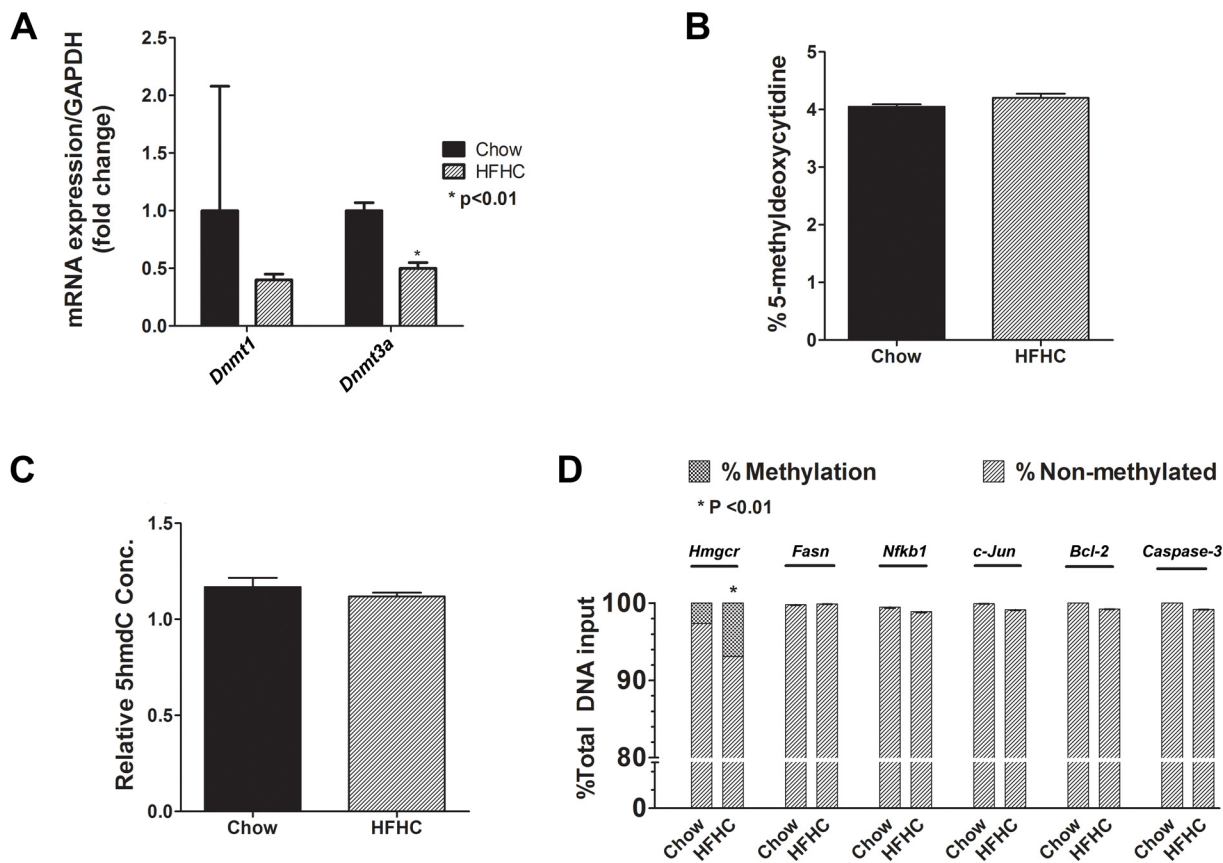

Fig 4. Stable global DNA methylation and hydroxymethylation and HMG-CoA reductase DNA hypermethylation in diet-induced NAFLD. (A-B) Although the gene expression for *Dnmt1* and *Dnmt3a* tended to decrease and decreased, respectively, the percent methyldeoxycytidine did not change between chow and HFHC group. (C) The relative 5hmdC concentrations also did not change. (D) Among the individual genes involved in the pathogenesis of NAFLD, *Hmgcr* was hypermethylated (p< 0.01) but there were no methylation changes for *Fasn*, *Nfkb1*, *c-Jun*, *Bcl-2*, and *Caspase 3* in HFHC group. Data are represented as mean ± SEM. Legend: B-cell lymphoma 2 (Bcl-2); DNA methyltransferase 1 and 3a (Dnmt 1 and Dnmt3a); fatty acid synthase (Fasn); 5-hydroxymethyl-2'-deoxycytidine (5hmdC); 3-hydroxy-3-methylglutaryl-coenzyme A reductase (HMG-CoA reductase, Hmgcr); nuclear factor of kappa light polypeptide gene enhancer in B-cells 1 (Nfkb1).
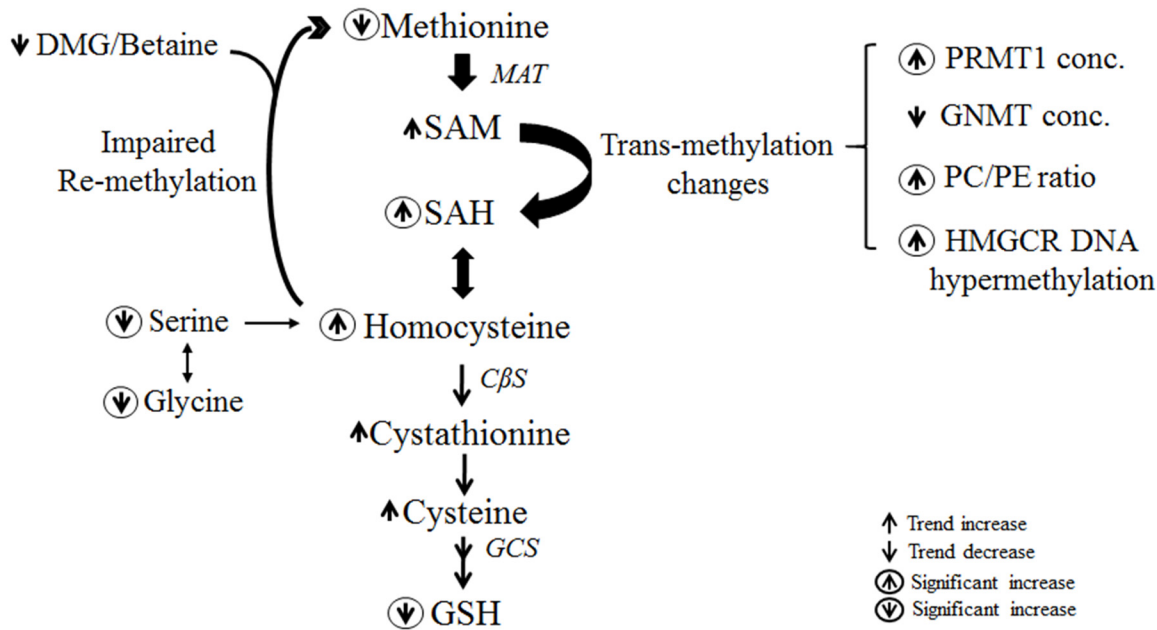
Fig 5. Summary of changes in the methionine cycle, transsulfuration pathway and methyltransferase reactions in advance NAFLD. HFHC diet for 52 weeks resulted in methionine depletion, excess homocysteine and aberrancy in transmethylation pathway. The decrease in the substrate serine impairs homocysteine remethylation and limits the ability to replete glutathione in the transsulfuration pathway. Legend: cystathionine β-synthase (CBS); dimethylglycine (DMG); γ-glutamylcysteine synthetase (GCS); glutathione (GSH); 3-hydroxy-3-methylglutaryl-coenzyme A reductase (HMGCR); methionine adenosyltransferase (MAT); phosphatidylcholine (PC); phosphatidylethanolamine (PE); protein arginine methytransferas 1 (PRMT1); s-adenosylmethionine (SAM); s-adenosylhomocysteine (SAH); s-adenosylhomocysteine hydrolase (SAHH).

doi:10.1371/journal.pone.0136822.g005

the observed methionine depletion despite an adequate diet suggests that the demand for methionine is a function of disease progression. The current study and available literature do not however inform us about whether the changes in methionine metabolic pathways reflect an adaptive response to limit disease progression or actually contribute to disease progression. This is an important consideration because an adaptive response would provide a rationale for methionine supplementation whereas a maladaptive response would not. It is therefore probably wise to perform additional preclinical trials of methionine supplementation before engaging in large scale human studies.

Hyperhomocysteinemia is closely associated with the metabolic syndrome and has been shown to be present in subjects with NAFLD [14–16]. It has been demonstrated that accumulation of homocysteine activates hepatic unfolded protein response and induces oxidative stress, hepatic inflammation and fibrosis [19, 20]. Homocysteine is an intermediate in methionine metabolism, which takes place mainly in the liver [9]. The observed depletion of methionine and increase in SAM and SAH suggests increased formation of hepatic homocysteine as a result of increased transmethylation activity of SAM. However, it is important to note that the levels of SAH hydrolase decreased excessively which do correlate with SAH elevation but not the increase in homocysteine. This suggests that homocysteine accumulation results from decreased in its utilization, either from altered remethylation to methionine and/or transsulfuration activity.

Remethylation of homocysteine requires the activity of methionine synthase and betaine-homocysteine methyltransferase and the availability of betaine and serine-dependent folate cycle activity [13, 37, 38]. The current study demonstrates that the expression of these enzymes is not significantly changed under conditions of a HFHC diet. However, there is a depletion of

serine which would be expected to impair transfer of methyl groups from methyltetrahydrofolate [38] and inhibit remethylation of homocysteine. The decreased dimethylglycine to betaine ratio is also supportive of the concept that impaired remethylation of homocysteine to methionine [39] contributes to methionine depletion as well as homocysteine elevation following long term administration of a HFHC diet and development of NAFLD with fibrosis. Impaired remethylation has also been suggested to be present in humans with NAFLD [21].

Providing substrates for critical enzymes in the transsulfuration pathway to replete glutathione would be expected to reduce homocysteine levels. This pathway is therefore unlikely to contribute to homocysteine elevation in NAFLD. It is already established that a high-fat diet is associated with oxidative stress and increased glutathione turnover [40–42]. In our study, there has been only a modest increase in cystathionine and cysteine levels despite a significant increase in homocysteine levels. It is known that homocysteine condenses with serine to form cystathionine, which is deaminated and hydrolyzed to form cysteine [43]. The fractional contribution of serine carbon to cysthathionine to meet the higher demands for glutathione has been demonstrated to be higher in NASH following intralipid infusion [44]. In addition, the levels of glycine, a substrate of serine, are also significantly decreased with long-term HFHC diet. In mammals, glycine is metabolized by the glycine cleavage system to form N_5N_{10} methylene-tetrahydrofolate (THF) [45]. Catalyzed by serine hydroymethyltransferase, glycine can form serine by transfer of the methyl group from THF [44]. It is therefore inferred that availability of cystathionine and cysteine to replete glutathione stores is limited by the reduction in the substrates, serine and glycine, under conditions of long-term HFHC diet. It is imperative to explore the supplementation of these substrates to treat NASH by restoring glutathione levels and reducing the concentration of homocysteine that plays an important role in NAFLD disease progression.

It is also attractive to hypothesize that increased demand for homocysteine to replete glutathione under conditions of diet-induced oxidative stress drives the demethylation of methionine and SAM and is a key driver for methionine depletion. If so, therapies associated with decreased oxidative stress and protection of glutathione stores would be expected to ameliorate the depletion of methionine. Of note, in humans with NASH, we have observed a trend for a decrease in circulating homocysteine levels after vitamin E treatment (unpublished data from metabolomic analyses of plasma samples of subjects in the PIVENS trial) [46].

The current study also provides evidence of aberrancy in methyltransferase reactions as a result of long-term HFHC diet. GNMT is the most abundant methyltransferase in the liver and mainly involved in hepatic SAM catabolism. In *Gnmt* knockout mice, SAM becomes elevated and results in rapid development of NAFLD [47]. In the current study, SAM is only modestly elevated despite decreased GNMT levels. It is possible that SAM is markedly being utilized by other methyltransferase reactions. An increase in PEMT flux as an adaptive response to hepatic SAM accumulation is observed in GNMT knockout mice [44]. The relative increase in PC (product) to PE (substrate) ratio in the present study despite a general depletion of these phospholipids suggests continued activity of this enzyme. The depletion of these phospholipids is also observed by our group in human NAFLD [48]. The decrease in PC in particular can potentially affect membrane fluidity and activate the unfolded protein response, playing a role in the pathogenesis of NAFLD. The lack of changes in choline levels argues against increased CDP-choline mediated PC synthesis, although a definitive statement about this cannot be made.

Interestingly, the methylated arginine metabolites (ADMA and MMA) were depleted from the liver in mice after the 52 week HFHC diet. This occurred despite a significant increase in the protein levels of PRMT1, which would be expected to drive increased formation of these compounds, along with increased circulating ADMA levels. We infer this to represent increased formation of ADMA and MMA and its export from hepatocytes. It is important to

note that ADMA is well known to inhibit nitric oxide synthase (NOS) activity and an important modulator of eNOS-mediated vasodilation [49, 50]. NAFLD has been associated with increased iNOS activity and inflammation and iNOS knockdown has been shown to ameliorate both inflammation and injury/apoptosis [51–54]. The depletion of hepatic ADMA in this study provides a potential mechanism for the increased iNOS observed by others under conditions of HFHC diet [52, 55]. Concomitantly, increased circulating ADMA is likely to contribute to systemic endothelial dysfunction commonly seen in NAFLD [56].

DNA methylation is an essential epigenetic mechanism and deoxycytidine methylation within CpG islands on promoters of genes inhibits transcriptional factor binding and, thus, generally inhibits gene expression [57, 58]. The development of hepatic steatosis in a mouse model was accompanied by altered expression of DNMT 1 and DNMT 3A in the liver [59]. In the current study, although the gene expression of *Dnmt3a* was significantly decreased, we did not observe any significant changes in global methylation status in mice fed with HFHC diet. Furthermore, the individual methylation of *Fasn*, *Nfkb1*, *c-Jun*, *Bcl-2* and *Caspase-3* were unchanged. Moreover, the individual methylation of FAS, NFkB1, c-Jun, Bcl-2 and caspase-3 were unchanged. Therefore, there was a lack of epigenetic adaptation to minimize de novo lipogenesis, inflammation and apoptosis in mice with NAFLD. The only potential exception is the observed hypermethylation of *Hmgcr* which likely represents an adaptive response to decrease cholesterol synthesis in the face of dietary cholesterol overload.

In summary, advanced NAFLD is associated with multiple alterations in methionine metabolism that lead to hepatic methionine deficiency and homocysteine elevation, mainly as a result of impaired remethylation of homocysteine to methionine. While high homocysteine levels provide substrate for glutathione repletion, this by itself may contribute to disease progression in NAFLD. The depletion of the substrate serine also limits the repletion of glutathione stores in response to oxidative stress. There is also aberrancy in methyltransferase reactions, as evidenced by decrease in *Gnmt* and increase in PC/PE ratio and PRMT. The decrease in ADMA and MMA levels plays an important mechanistic role in NAFLD pathogenesis by increasing iNOS-mediated inflammation and apoptosis, thus, disease progression in NAFLD.

Supporting Information

S1 Fig. Representative image of steatosis induced by a high-fat high-calorie diet for 52 weeks. Liver tissues were stained with hematoxylin and eosin (HE). In high-power field, macrovesicular steatosis and small droplet steatosis, which is centrilobular in distribution, was present in the liver under conditions of high-fat high-calorie diet for 52 weeks (**1a**).
(TIF)

S2 Fig. Representative image of inflammation and fibrosis induced by a high-fat high-calorie diet for 52 weeks. Liver tissues from mice fed a high-fat high-calorie diet for 52 weeks were stained with Masson's trichrome stain. Scattered foci of inflammatory cells and extensive pericellular fibrosis were observed, indicating an advanced form of NAFLD.
(TIF)

S1 Table. MAT, methionine adenosyltransferase; Ahcy, adenosylhomocysteinase; Gnmt, glycine N-methyltransferase; Cbs, cystathionine β-synthase; γ-Gcs, γ-glutamylcysteine synthetase; Bhmt, betaine-homocysteine methyltransferase; Ms, methionine synthase; Prmt, protein arginine methyltransferase; Dnmt, DNA methyltransferase; Gapdh, glyceraldehyde 3-phosphate dehydrogenase.
(DOCX)

Author Contributions

Conceived and designed the experiments: TP AJS EQ. Performed the experiments: TP SC EQ. Analyzed the data: TP SC AV VP HM FM EQ AJS. Contributed reagents/materials/analysis tools: TP SC AV EQ HM FM AJS. Wrote the paper: TP SC AJS.

References

1. Lazo M, Clark JM. The epidemiology of nonalcoholic fatty liver disease: a global perspective. Semin Liver Dis. 2008; 28(4):339–50. doi: 10.1055/s-0028-1091978 PMID: 18956290

2. Vanni E, Bugianesi E, Kotronen A, De Minicis S, Yki-Jarvinen H, Svegliati-Baroni G. From the metabolic syndrome to NAFLD or vice versa? Dig Liver Dis. 2010; 42(5):320–30. doi: 10.1016/j.dld.2010.01.016 PMID: 20207596

3. Bugianesi E, Moscatiello S, Ciaravella MF, Marchesini G. Insulin resistance in nonalcoholic fatty liver disease. Curr Pharm Des. 2010; 16(17):1941–51. PMID: 20370677

4. Soderberg C, Stal P, Askling J, Glaumann H, Lindberg G, Marmur J, et al. Decreased survival of subjects with elevated liver function tests during a 28-year follow-up. Hepatology. 2010; 51(2):595–602. doi: 10.1002/hep.23314 PMID: 20014114

5. Rafiq N, Bai C, Fang Y, Srishord M, McCullough A, Gramlich T, et al. Long-term follow-up of patients with nonalcoholic fatty liver. Clin Gastroenterol Hepatol. 2009; 7(2):234–8. doi: 10.1016/j.cgh.2008.11.005 PMID: 19049831

6. Lazo M, Hernaez R, Bonekamp S, Kamel IR, Brancati FL, Guallar E, et al. Non-alcoholic fatty liver disease and mortality among US adults: prospective cohort study. BMJ. 2011; 343:d6891. doi: 10.1136/bmj.d6891 PMID: 22102439

7. Mato JM, Martinez-Chantar ML, Lu SC. Methionine metabolism and liver disease. Annu Rev Nutr. 2008; 28:273–93. doi: 10.1146/annurev.nutr.28.061807.155438 PMID: 18331185

8. Finkelstein JD. Methionine metabolism in liver diseases. Am J Clin Nutr. 2003; 77(5):1094–5. PMID: 12716657

9. Garcia-Tevijano ER, Berasain C, Rodriguez JA, Corrales FJ, Arias R, Martin-Duce A, et al. Hyperhomocysteinemia in liver cirrhosis: mechanisms and role in vascular and hepatic fibrosis. Hypertension. 2001; 38(5):1217–21. PMID: 11711526

10. Stead LM, Brosnan JT, Brosnan ME, Vance DE, Jacobs RL. Is it time to reevaluate methyl balance in humans? Am J Clin Nutr. 2006; 83(1):5–10. PMID: 16400042

11. Bedford MT. Arginine methylation at a glance. J Cell Sci. 2007; 120(Pt 24):4243–6. doi: 10.1242/jcs.019885 PMID: 18057026

12. Mato JM, Lu SC. Role of S-adenosyl-L-methionine in liver health and injury. Hepatology. 2007; 45(5):1306–12. doi: 10.1002/hep.21650 PMID: 17464973

13. Williams KT, Schalinske KL. Homocysteine metabolism and its relation to health and disease. Biofactors. 2010; 36(1):19–24. doi: 10.1002/biof.71 PMID: 20091801

14. Gulsen M, Yesilova Z, Bagci S, Uygun A, Ozcan A, Ercin CN, et al. Elevated plasma homocysteine concentrations as a predictor of steatohepatitis in patients with non-alcoholic fatty liver disease. J Gastroenterol Hepatol. 2005; 20(9):1448–55. doi: 10.1111/j.1440-1746.2005.03891.x PMID: 16105135

15. Hajer GR, van der Graaf Y, Olijhoek JK, Verhaar MC, Visseren FL, Group SS. Levels of homocysteine are increased in metabolic syndrome patients but are not associated with an increased cardiovascular risk, in contrast to patients without the metabolic syndrome. Heart. 2007; 93(2):216–20. doi: 10.1136/hrt.2006.093971 PMID: 16952974

16. de Carvalho SC, Muniz MT, Siqueira MD, Siqueira ER, Gomes AV, Silva KA, et al. Plasmatic higher levels of homocysteine in non-alcoholic fatty liver disease (NAFLD). Nutr J. 2013; 12:37. doi: 10.1186/1475-2891-12-37 PMID: 23547829

17. Austin RC, Lentz SR, Werstuck GH. Role of hyperhomocysteinemia in endothelial dysfunction and atherothrombotic disease. Cell Death Differ. 2004; 11 Suppl 1:S56–64. doi: 10.1038/sj.cdd.4401451 PMID: 15243582

18. Refsum H, Ueland PM, Nygard O, Vollset SE. Homocysteine and cardiovascular disease. Annu Rev Med. 1998; 49:31–62. doi: 10.1146/annurev.med.49.1.31 PMID: 9509248

19. Henkel AS, Elias MS, Green RM. Homocysteine supplementation attenuates the unfolded protein response in a murine nutritional model of steatohepatitis. J Biol Chem. 2009; 284(46):31807–16. doi: 10.1074/jbc.M109.017970 PMID: 19762918

20. Matte C, Stefanello FM, Mackedanz V, Pederzolli CD, Lamers ML, Dutra-Filho CS, et al. Homocysteine induces oxidative stress, inflammatory infiltration, fibrosis and reduces glycogen/glycoprotein content in liver of rats. Int J Dev Neurosci. 2009; 27(4):337–44. doi: 10.1016/j.ijdevneu.2009.03.005 PMID: 19460627

21. Kalhan SC, Edmison J, Marczewski S, Dasarathy S, Gruca LL, Bennett C, et al. Methionine and protein metabolism in non-alcoholic steatohepatitis: evidence for lower rate of transmethylation of methionine. Clin Sci (Lond). 2011; 121(4):179–89. doi: 10.1042/CS20110060

22. Kwon do Y, Jung YS, Kim SJ, Park HK, Park JH, Kim YC. Impaired sulfur-amino acid metabolism and oxidative stress in nonalcoholic fatty liver are alleviated by betaine supplementation in rats. J Nutr. 2009; 139(1):63–8. doi: 10.3945/jn.108.094771 PMID: 19056644

23. Yun KU, Ryu CS, Oh JM, Kim CH, Lee KS, Lee CH, et al. Plasma homocysteine level and hepatic sulfur amino acid metabolism in mice fed a high-fat diet. Eur J Nutr. 2013; 52(1):127–34. doi: 10.1007/s00394-011-0294-0 PMID: 22209966

24. Rubio-Aliaga I, Roos B, Sailer M, McLoughlin GA, Boekschoten MV, van Erk M, et al. Alterations in hepatic one-carbon metabolism and related pathways following a high-fat dietary intervention. Physiol Genomics. 2011; 43(8):408–16. doi: 10.1152/physiolgenomics.00179.2010 PMID: 21303933

25. Dahlhoff C, Desmarchelier C, Sailer M, Furst RW, Haag A, Ulbrich SE, et al. Hepatic methionine homeostasis is conserved in C57BL/6N mice on high-fat diet despite major changes in hepatic one-carbon metabolism. PLoS One. 2013; 8(3):e57387. doi: 10.1371/journal.pone.0057387 PMID: 23472083

26. Puri P, Mirshahi F, Cheung O, Natarajan R, Maher JW, Kellum JM, et al. Activation and dysregulation of the unfolded protein response in nonalcoholic fatty liver disease. Gastroenterology. 2008; 134 (2):568–76. doi: 10.1053/j.gastro.2007.10.039 PMID: 18082745

27. Cheung O, Puri P, Eicken C, Contos MJ, Mirshahi F, Maher JW, et al. Nonalcoholic steatohepatitis is associated with altered hepatic MicroRNA expression. Hepatology. 2008; 48(6):1810–20. doi: 10.1002/hep.22569 PMID: 19030170

28. Araki A, Sako Y. Determination of free and total homocysteine in human plasma by high-performance liquid chromatography with fluorescence detection. J Chromatogr. 1987; 422:43–52. PMID: 3437026

29. FJ W. Biomarker methods in drug discovery and development. Totowa, Nj: Humana Press. 2008.

30. Stahlman M, Ejsing CS, Tarasov K, Perman J, Boren J, Ekroos K. High-throughput shotgun lipidomics by quadrupole time-of-flight mass spectrometry. J Chromatogr B Analyt Technol Biomed Life Sci. 2009; 877(26):2664–72. doi: 10.1016/j.jchromb.2009.02.037 PMID: 19286428

31. Ekroos K, Ejsing CS, Bahr U, Karas M, Simons K, Shevchenko A. Charting molecular composition of phosphatidylcholines by fatty acid scanning and ion trap MS3 fragmentation. J Lipid Res. 2003; 44 (11):2181–92. doi: 10.1194/jlr.D300020-JLR200 PMID: 12923235

32. Ekroos K, Chernushevich IV, Simons K, Shevchenko A. Quantitative profiling of phospholipids by multiple precursor ion scanning on a hybrid quadrupole time-of-flight mass spectrometer. Anal Chem. 2002; 74(5):941–9. PMID: 11924996

33. Quinlivan EP, Gregory JF 3rd. DNA methylation determination by liquid chromatography-tandem mass spectrometry using novel biosynthetic [U-15N]deoxycytidine and [U-15N]methyldeoxycytidine internal standards. Nucleic Acids Res. 2008; 36(18):e119. doi: 10.1093/nar/gkn534 PMID: 18718928

34. Quinlivan EP, Gregory JF 3rd. DNA digestion to deoxyribonucleoside: a simplified one-step procedure. Anal Biochem. 2008; 373(2):383–5. doi: 10.1016/j.ab.2007.09.031 PMID: 18028864

35. Lu SC, Mato JM. S-Adenosylmethionine in cell growth, apoptosis and liver cancer. J Gastroenterol Hepatol. 2008; 23 Suppl 1:S73–7. doi: 10.1111/j.1440-1746.2007.05289.x PMID: 18336669

36. Cook RJ. Defining the steps of the folate one-carbon shuffle and homocysteine metabolism. Am J Clin Nutr. 2000; 72(6):1419–20. PMID: 11101465

37. Gregory JF 3rd, Cuskelly GJ, Shane B, Toth JP, Baumgartner TG, Stacpoole PW. Primed, constant infusion with [2H3]serine allows in vivo kinetic measurement of serine turnover, homocysteine remethylation, and transsulfuration processes in human one-carbon metabolism. Am J Clin Nutr. 2000; 72 (6):1535–41. PMID: 11101483

38. Davis SR, Stacpoole PW, Williamson J, Kick LS, Quinlivan EP, Coats BS, et al. Tracer-derived total and folate-dependent homocysteine remethylation and synthesis rates in humans indicate that serine is the main one-carbon donor. Am J Physiol Endocrinol Metab. 2004; 286(2):E272–9. doi: 10.1152/ajpendo.00351.2003 PMID: 14559726

39. Kathirvel E, Morgan K, Nandgiri G, Sandoval BC, Caudill MA, Bottiglieri T, et al. Betaine improves non-alcoholic fatty liver and associated hepatic insulin resistance: a potential mechanism for hepatoprotection by betaine. Am J Physiol Gastrointest Liver Physiol. 2010; 299(5):G1068–77. doi: 10.1152/ajpgi.00249.2010 PMID: 20724529

40. Rolo AP, Teodoro JS, Palmeira CM. Role of oxidative stress in the pathogenesis of nonalcoholic steato-hepatitis. Free Radic Biol Med. 2012; 52(1):59–69. doi: 10.1016/j.freeradbiomed.2011.10.003 PMID: 22064361

41. Videla LA, Rodrigo R, Orellana M, Fernandez V, Tapia G, Quinones L, et al. Oxidative stress-related parameters in the liver of non-alcoholic fatty liver disease patients. Clin Sci (Lond). 2004; 106(3):261–8. doi: 10.1042/CS20030285

42. Carmiel-Haggai M, Cederbaum AI, Nieto N. A high-fat diet leads to the progression of non-alcoholic fatty liver disease in obese rats. FASEB J. 2005; 19(1):136–8. doi: 10.1096/fj.04-2291fje PMID: 15522905

43. Wang L, Jhee KH, Hua X, DiBello PM, Jacobsen DW, Kruger WD. Modulation of cystathionine beta-synthase level regulates total serum homocysteine in mice. Circ Res. 2004; 94(10):1318–24. doi: 10.1161/01.RES.0000129182.46440.4a PMID: 15105297

44. Dasarathy S, Kasumov T, Edmison JM, Gruca LL, Bennett C, Duenas C, et al. Glycine and urea kinetics in nonalcoholic steatohepatitis in human: effect of intralipid infusion. Am J Physiol Gastrointest Liver Physiol. 2009; 297(3):G567–75. doi: 10.1152/ajpgi.00042.2009 PMID: 19571235

45. Kikuchi G, Motokawa Y, Yoshida T, Hiraga K. Glycine cleavage system: reaction mechanism, physiological significance, and hyperglycinemia. Proc Jpn Acad Ser B Phys Biol Sci. 2008; 84(7):246–63. PMID: 18941301

46. Cheng J, Joyce A, Yates K, Aouizerat B, Sanyal AJ. Metabolomic profiling to identify predictors of response to vitamin E for non-alcoholic steatohepatitis (NASH). PLoS One. 2012; 7(9):e44106. doi: 10.1371/journal.pone.0044106 PMID: 23028489

47. Martinez-Chantar ML, Vazquez-Chantada M, Ariz U, Martinez N, Varela M, Luka Z, et al. Loss of the glycine N-methyltransferase gene leads to steatosis and hepatocellular carcinoma in mice. Hepatology. 2008; 47(4):1191–9. doi: 10.1002/hep.22159 PMID: 18318442

48. Puri P, Baillie RA, Wiest MM, Mirshahi F, Choudhury J, Cheung O, et al. A lipidomic analysis of nonalcoholic fatty liver disease. Hepatology. 2007; 46(4):1081–90. doi: 10.1002/hep.21763 PMID: 17654743

49. Forstermann U, Sessa WC. Nitric oxide synthases: regulation and function. Eur Heart J. 2012; 33 (7):829–37, 37a–37d. doi: 10.1093/eurheartj/ehr304 PMID: 21890489

50. Sibal L, Agarwal SC, Home PD, Boger RH. The Role of Asymmetric Dimethylarginine (ADMA) in Endothelial Dysfunction and Cardiovascular Disease. Curr Cardiol Rev. 2010; 6(2):82–90. doi: 10.2174/157340310791162659 PMID: 21532773

51. Spruss A, Kanuri G, Uebel K, Bischoff SC, Bergheim I. Role of the inducible nitric oxide synthase in the onset of fructose-induced steatosis in mice. Antioxid Redox Signal. 2011; 14(11):2121–35. doi: 10.1089/ars.2010.3263 PMID: 21083420

52. Wan G, Ohnomi S, Kato N. Increased hepatic activity of inducible nitric oxide synthase in rats fed on a high-fat diet. Biosci Biotechnol Biochem. 2000; 64(3):555–61. doi: 10.1271/bbb.64.555 PMID: 10803953

53. Sass G, Koerber K, Bang R, Guehring H, Tiegs G. Inducible nitric oxide synthase is critical for immune-mediated liver injury in mice. J Clin Invest. 2001; 107(4):439–47. doi: 10.1172/JCI10613 PMID: 11181643

54. Fujita K, Nozaki Y, Yoneda M, Wada K, Takahashi H, Kirikoshi H, et al. Nitric oxide plays a crucial role in the development/progression of nonalcoholic steatohepatitis in the choline-deficient, l-amino acid-defined diet-fed rat model. Alcohol Clin Exp Res. 2010; 34 Suppl 1:S18–24. doi: 10.1111/j.1530-0277.2008.00756.x PMID: 18986378

55. Ha SK, Chae C. Inducible nitric oxide distribution in the fatty liver of a mouse with high fat diet-induced obesity. Exp Anim. 2010; 59(5):595–604. PMID: 21030787

56. Kasumov T, Edmison JM, Dasarathy S, Bennett C, Lopez R, Kalhan SC. Plasma levels of asymmetric dimethylarginine in patients with biopsy-proven nonalcoholic fatty liver disease. Metabolism. 2011; 60 (6):776–81. doi: 10.1016/j.metabol.2010.07.027 PMID: 20869086

57. Robertson KD. DNA methylation and human disease. Nat Rev Genet. 2005; 6(8):597–610. PMID: 16136652

58. Jones PA. Functions of DNA methylation: islands, start sites, gene bodies and beyond. Nat Rev Genet. 2012; 13(7):484–92. doi: 10.1038/nrg3230 PMID: 22641018

59. Pogribny IP, Tryndyak VP, Bagnyukova TV, Melnyk S, Montgomery B, Ross SA, et al. Hepatic epigenetic phenotype predetermines individual susceptibility to hepatic steatosis in mice fed a lipogenic methyl-deficient diet. J Hepatol. 2009; 51(1):176–86. doi: 10.1016/j.jhep.2009.03.021 PMID: 19450891